Cloud Publications
International Journal of Advanced Remote Sensing and GIS
2017, Volume 6, Issue 1, pp. 2171-2177
ISSN 2320 – 0243, Crossref: 10.23953/cloud.ijarsg.264

Research Article

Lithologic Mapping using Remote Sensing Data in Abu Marawat Area, Eastern Desert of Egypt

Mohamed Abdelkareem[1], Ibrahim Othman[2], Kamal El Din G[1]

[1]Geology Department, South Valley University, Egypt
[2]Egyptian Company for Mineral Resources, Egypt

Publication Date: 30 May 2017

DOI: https://doi.org/10.23953/cloud.ijarsg.264

Abstract Remotely sensing data include Landsat-8 Operational Land Imager (OLI) and Advanced Spaceborne Thermal Emission and Reflection Radiometer (ASTER) data successfully delineated the alteration zone in Abu Marawat area. Image transformation technique was applied in the present study. Band ratio color composites (6/7, 6/5,*4/5, 5) and Principal Component Analysis (PCA) technique of Landsat-8 highlighted the alteration zone. Band ratio color composites ASTER bands 4/6, 4/2, and 4/3 in the R, G, and B, respectively, provided a significant results of alteration zone. Minimum Noise fraction technique (MNF) provided better results that clearly delineated the mineral potential area. Field data and previous works validated the alteration zones. The overall results showed the importance of image processing in showing the probable area of mineral resources.
Keywords *Remote sensing, image processing, alteration zone; Egypt*

1. Introduction

Advances in multispectral imaging systems include Landsat series and Advanced Spaceborne Thermal Emission and Reflection Radiometer (ASTER) allowed mapping the geologic and structural features in fine resolutions (e.g., Abdelkareem and El-Baz, 2015 & 2016 & 2017). Landsat sensors (e.g., Landsat-5 to Landsat-8) successfully delineated lithologic and mineral characteristics using visible NIR and SWIR bands (e.g., Abrams et al., 1983; Sabins, 1997; Ramadan et al., 2004). On February 11, 2013 the new Landsat Operational Land Imager (OLI) which aboard by Landsat-8 improved the spectral, radiometric and spatial resolutions of the acquired data. This sensor measures the reflected electromagnetic waves in nine bands and measures the Thermal wavelengths in two bands (TIR). Several studies were used the OLI in imaging the hydrothermal alteration minerals (Zhang et al., 2016; Pour and Hashim, 2015; Abdelkareem and El-Baz, 2016).

ASTER aboard the Earth observation system (EOS) Terra platform measures the Electromagnetic (EM) waves in 14 spectral bands. This sensor has the advantage to cover the SWIR which are significant to map several mineral groups include hydroxides, hydrates and carbonates (Abdelkareem and El-Baz, 2016). This allowed discriminating between key-alteration minerals such as kaolinite, smectite, alunite, and jarosite (Zhang et al., 2016; Yamaguchi and Naito, 2003; Pour and Hashim, 2012; Rowan et al., 2003; Hubbard and Crowley, 2005; Zadeh et al., 2014). These minerals of alteration zones appear on contact with ore deposits which occupied the center of the alteration zones. Analysis and integration of OLI and ASTER data are effective in predicting the occurrence of a certain

group of minerals; Al-OH, Fe-OH and Mg-OH e.g., kaolinite, alunite, illite, muscovite, montmorillonite, chlorite, calcite, and dolomite (Azizi et al., 2010; Mars and Rowan, 2006; Rowan et al., 2006).

Several studies were carried out in the Central Eastern Desert of Egypt to map lithology and alteration zone (e.g., Sultan et al., 1986 & 1987; Gabr et al., 2010; Asran et al., 2012; Kusky and Ramadan, 2002). The aim of the present study is to apply OLI and ASTER data to map and highlight area of hydrothermal alteration zones as an indication of mineral resources in the arid regions.

2. Study Area

Abu Marawat area is located in the northern portion of the Central Eastern Desert of Egypt (Figure 1). Regionally, the geology of the studied area consists of ultramafic rocks (Serpentinite-talc-carbonate rocks) which represent the oldest geologic unit, overlain by island arc-related metavolcano-sedimentary sequences. These rock units overlain by Hammamat sediments and intruded by a variety of granitic rocks. These varieties cut by dykes and quartz veins that occur as a later phase of magmatic intrusion.

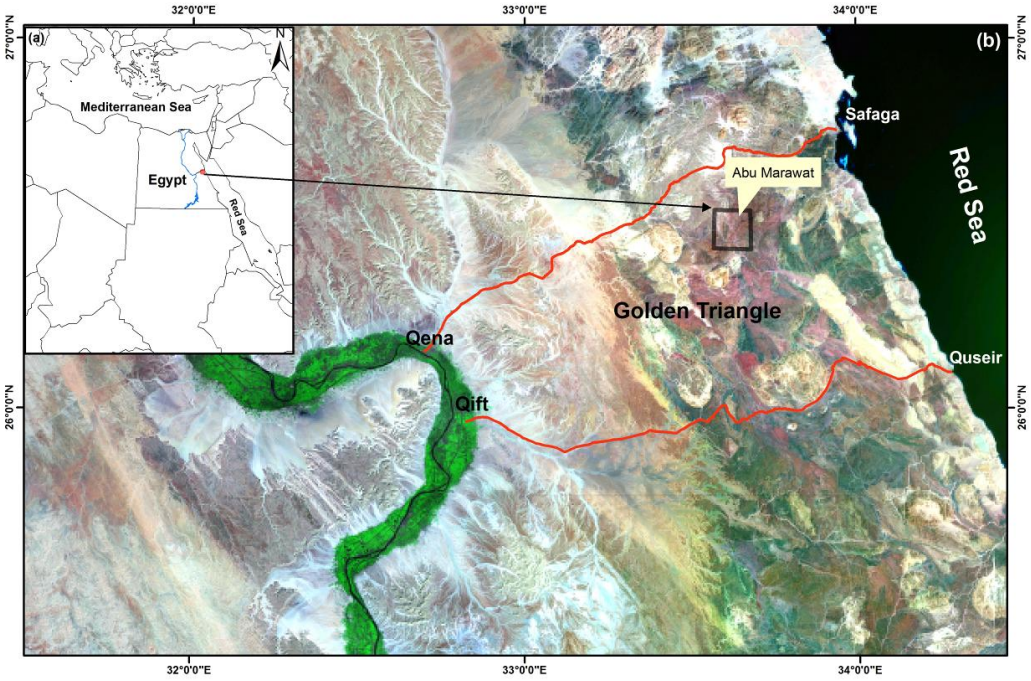

Figure 1: *Location map of the study area*

3. Data Used and Methods

Landsat-8 (OLI) and ASTER data were used in the present study. The OLI has nine optical bands and two bands measure the Thermal IR wavelengths. The OLI bands 2, 3, 4, 5, 6 and 7 are processed and transformed in the present study. The OLI sensor collect two sub-systems visible near infrared (VNIR); shortwave infrared (SWIR), and Thermal infrared (TIR). The spatial coverage of VNIR and SWIR is 30 m and, the TIR is about 60 m. Image enhancement, and transformations were used to delineate the areas of mineral alteration zone. In addition to OLI data, ASTER data which obtained in December 1999 by NASA and METT (Japan Ministry of Economic trade and industry) were used to highlight areas of hydrothermal alterations. The data were georeferenced to Universal Transverse Mercator (UTM). World Geodetic system 1984 (WGS 84) zone 36.

Band ratio represents a transformation technique that applies by dividing the digital numbers of one band by their corresponding pixels of another band (e.g., Mather, 2004). This helps to enhance the spectral differences between the variables on land surface (Goetz et al., 1983). This technique allowed discrimination between different rock types and highlighted areas rich in specific mineral compositions (Abrams et al., 1983; Sabins 1997; Abdelkareem and El-Baz, 2016; Gad and Kusky, 2006). In addition to band ratios, PCA was used to transform the components of the image into its principal components (Loughlin, 1991; Gomez et al., 2005). This transformation has the ability to highlight the similarities and differences in the used data. The output will be eigenvectors and eigenvalues of the matrix Covariance.

Minimum noise transformation technique also was used to segregate noise from the VNIR-SWIR ASTER Data. The advantage of this technique is to filter or remove those bands that contribute most to noise (Green et al., 1988; Boardman and Kruse, 1994). It is better technique than PCA in compressing and ordering data in relationship of their image quality. Where the PCA technique is yields linear transformations of the input data which subsequently amplify their variance, and the MNF transform yields linear transformation which subsequently reduce their noise fraction.

4. Results and Discussion

4.1. Landsat-8

Using band ratios 6/7, 6/5,*4/5, 5 in R, G, B (Figure 2a) allowed discriminating geologic units such as felsic varieties with pinkish color; however, the mafic-intermediate rocks discriminated in greenish color. This is because iron oxides and iron-bearing minerals are highlighted by band ratios 6/5,*4/5 (Sultan, 1986 & 1987). The alteration zones could be identified by their yellow/whitish yellow color. This composite discriminated the mineralized alteration zone in bright yellow tone whitish yellow colors from all the others rock units.

Using PCA transformation (Table 1), it is found that band 6 contributed more than the other bands. The eigenvalue of the first PC represents 95.24% of the total variance. This component have negative loading from all bands. The second principle component “PC2” displays contrast between the VNIR and SWIR bands. Noteworthy, PC3 displays contrast between band 6 (0.601736) and band 7 (-0.61628) that provides significant information on the OH-bearing minerals. In PC5, a contrast between band 4 (0.811358) and band 2 (-0.24045) that reveal the iron oxides in bright tone. In this transformation, the PC6 represents noise. Displaying PC3, PC4, and PC5 in R, G, and B, (Figure 2b) allowed discriminating mineralized alteration zone with bright tone (reddish white color).

Table 1: *Principal component analysis of VNIR/SWIR*

Eigenvector	Band 2	Band 3	Band 4	Band 5	Band 6	Band 7	Eigenvalue%
St. dev	783.03	1194.90	1636.59	2022.79	2514.65	2150.75	
PC 1	-0.17	-0.26	-0.37	-0.45	-0.57	-0.48	95.24
PC 2	0.25	0.34	0.42	0.44	-0.38	-0.55	3.31
PC 3	-0.29	-0.29	-0.12	0.27	0.60	-0.61	0.95
PC 4	0.41	0.45	0.03	-0.62	0.40	-0.29	0.43
PC 5	-0.38	-0.24	0.81	-0.37	0.01	-0.01	0.052
PC 6	0.71	-0.68	0.13	0.0002	0.026	-0.006	0.017

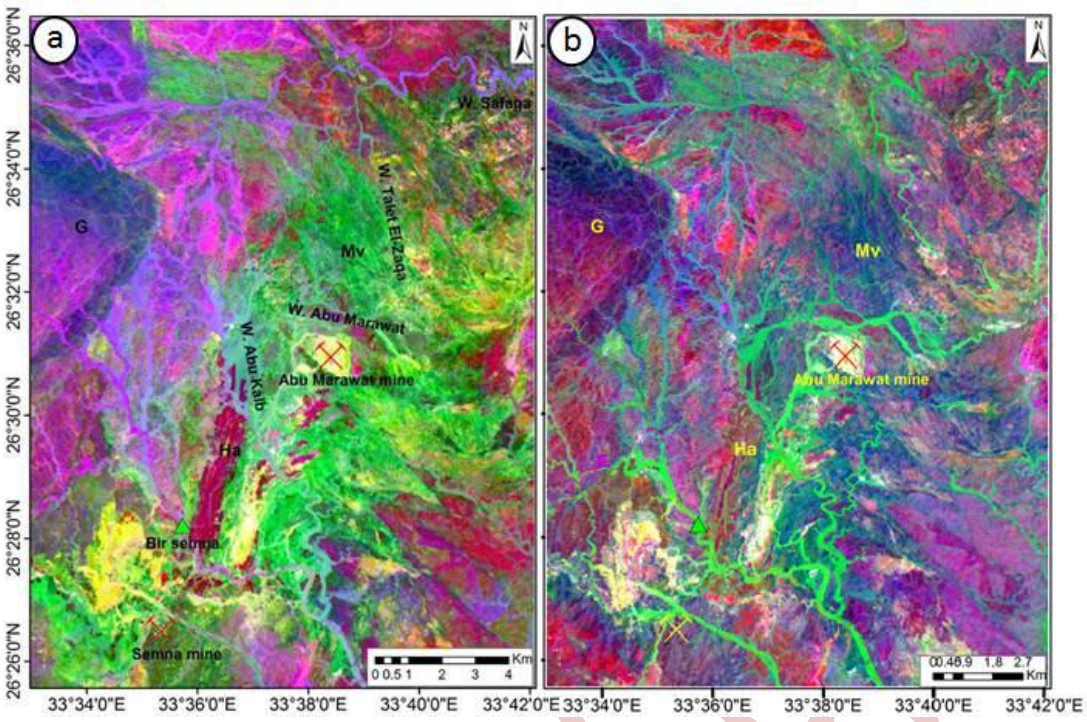

Figure 2: *(a) Band ratio composite image of 6/7, 6/5*4/5, 5 in R, G, and B. (b) False color composite of PC3, PC4, and PC5 in R, G, and B, respectively*

4.2. ASTER Data

Band ratio composite 4/6, 4/2, and 4/3 were used to enhance the spectral differences between altered and non-altered rocks. We apply band ratios 4/6 to highlight the aluminum hydroxide (Al-O-H), 4/2 and 4/3 for iron oxides. This based on that the spectral properties of hydrothermal alteration minerals are different from unaltered minerals. In areas of hydrothermal alteration, the OH- and iron bearing minerals are common. Therefore, using band ratios 4/6, 4/2, and 4/3 (Figure 3a) clearly highlighted the alteration minerals in bright white tone color.

The result of MNF technique which was applied on the VNIR-SWIR ASTER bands is shown in Figure 3b. This technique provides images with successive increasing noise level and decreasing image quality with increasing the fraction level (order). By examine the Minimum noise fraction output images; negated MNF4 represented the best component that highlighted the alteration zone clearly in white color (Figure 3b). Field examination (Figure 4) revealed the alteration zone and the detected sites are of high mineral potentials that represents the mine of Abu-Marawat.

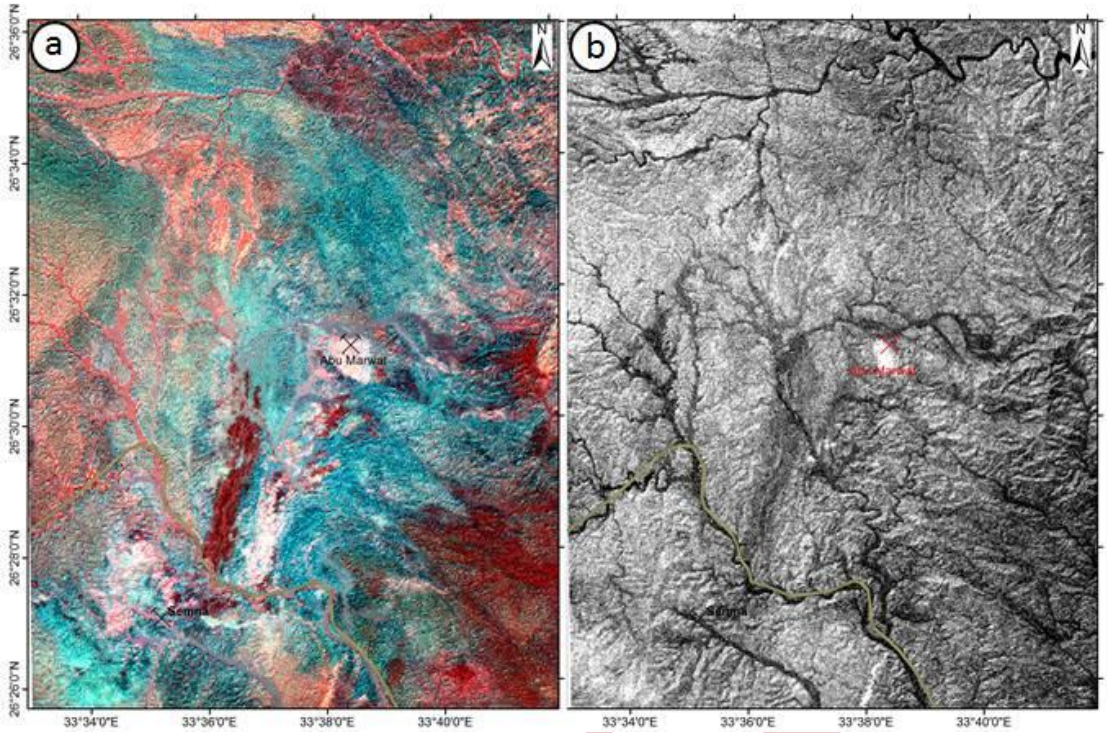

Figure 3: *(a) Band ratio composite image of 4/6, 4/2, 4/3 in R, G, and B. (b) MNF 4 of VNIR-SWIR ASTER bands*

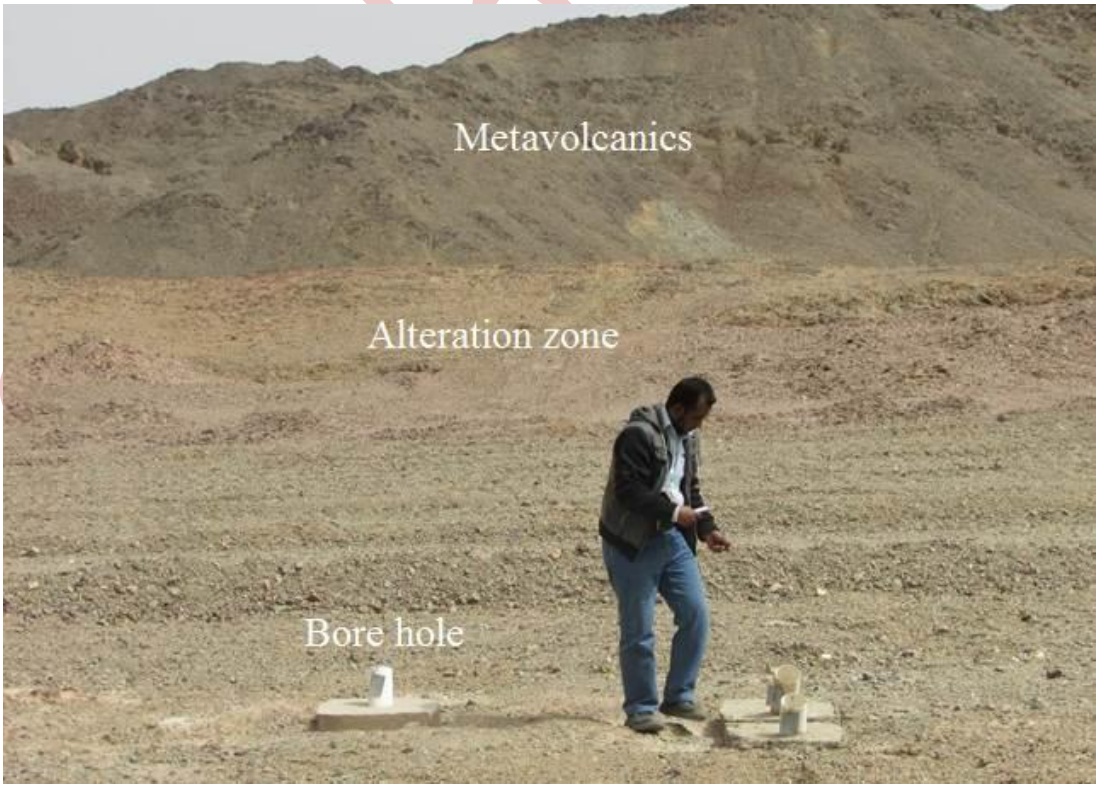

Figure 4: *Field photograph showing the alteration zone*

5. Conclusions

This article represents application of remote sensing data in arid region to characterize the hydrothermal alteration zone. OLI and ATER data clearly highlighted the potential area of hydrothermal alteration using image transformation technique. Applied the Minimum Noise Fraction provided better observation than band ratios and PCA in delineating the areas of hydrothermal alteration. In summary, applying remote sensing data is effective tool prior to any field investigations.

Acknowledgments

This article was funded by the South Valley University sector of Postgraduate Studies and Research.

References

Abdelkareem, El-Baz, F. 2016. Mapping hydrothermal alteration zone as a probable site of potential mineral resources in the Central Eastern Desert of Egypt using remotely-sensed data. *Geological Society of America Abstracts with Programs*, 48(7). doi: 10.1130/abs/2016AM-282399.

Abdelkareem, El-Baz, F. 2015. Analyses of optical images and radar data reveal structural features and predict groundwater accumulations in the central Eastern Desert of Egypt. *Arabian Journal of Geosciences*, 8, pp.2653-2666.

Abdelkareem, M. and El-Baz, F. Forthcoming 2017. Characterizing hydrothermal alteration zones in Hamama area in the central Eastern Desert of Egypt by remotely sensed data. *Journal of Geocarto International.* http://dx.doi.org/10.1080/10106049.2017.1325410

Abrams, M.J., Brown, D., Leple, L. and Sadowski, R. 1983. Remote sensing of porphyry copper deposits in Southern Arizona. *Economic Geology*, 78, pp.591-604.

Azizi, H., Tarverdi, M.A., and Akbarpour, A. 2010. Extraction of hydrothermal alterations from ASTER SWIR data from east Zanjan, northern Iran. *Advances in Space Research*, 46, pp.99-109.

Boardman, J.W. and Kruse F.A. 1994. Automated spectral analysis: a geologic example using AVIRIS data, north Grapevine Mountains, Nevada. In: *Proceedings, ERIM tenth thematic conference on geologic remote sensing*, 9-12 May 1994, San Antonio, Texas. Ann Arbor, MI: Environmental Research Institute of Michigan, pp.407-418.

Gabr, S., Ghulam, A. and Kusky, T. 2010. Detecting areas of high-potential gold mineralization using ASTER data. *Ore Geology Reviews*, 38, pp.59-69.

Gad, S. and Kusky, T. 2006. Lithological mapping in the Eastern Desert of Egypt, the Barramiya area, using Landsat thematic mapper (TM). *Journal of African Earth Sciences*, 44(2), pp.196-202.

Goetz, A.F.H., Rock, B.N. and Rowan, L.C. 1983. Remote sensing for exploration: an overview. *Economic Geology*, 78, 573-590.

Gomez, C., Delacourt, C., Allemand, P., Ledru, P. and Wackerle, R., 2005. Using ASTER remote sensing data set for geological mapping, in Namibia. *Physics and Chemistry of the Earth*, *parts A/B/C*, 30(1-3), pp.97-108.

Green, A.A., Berman, M., Switzer, P. and Craig, M.D. 1988. A transformation for ordering multispectral data in terms of image quality with implications for noise removal. *IEEE Transactions on Geoscience and Remote Sensing*, 26, pp.65-74.

Hubbard, B.E. and Crowley, J.K. 2005. Mineral mapping on the Chilean-Bolivian Altiplano using co-orbital ALI, ASTER and Hyperion imagery: Data dimensionality issues and solutions. *Remote Sensing of Environment*, 99, pp.173-186.

Kusky, T.M. and Ramadan, T.M. 2002. Structural controls in the Neoproterozoic Allaqi suture: An integrated field, Landsat TM, and radar C/X SIR SAR images. *Journal of African Earth Sciences*, 35, pp.107-121.

Loughlin, W.P. 1991. Principal component analysis for alteration mapping. *Photogrammetric Engineering and Remote Sensing*, 57, pp.1163-1169.

Mars, J.C. and Rowan, L.C. 2006. Regional mapping of phyllic- and argillic-altered rocks in the Zagros magmatic arc, Iran, using advanced spaceborne thermal emission and reflection radiometer (ASTER) data and logical operator algorithms. *Geosphere*, 2, pp.161-186.

Mather, P. 2004. *Computer Processing of Remotely-Sensed Images: An introduction*, 3rd Edition, Wiley, p.442.

Pour, A.B. and Hashim, M. 2015. Hydrothermal alteration mapping from Landsat-8 data, SarCheshmeh copper mining district, south-eastern Islamic Republic of Iran. Journal of Taibah University for Science, 9, pp.155-166.

Pour, A.B. and Hashim, M. 2012. Identifying areas of high economic-potential copper mineralization using ASTER data in the Urumieh-Dokhtar Volcanic Belt, Iran. Advances in Space Research, 49, pp.753-769.

Rowan, L.C., Mars, J.C. and Simpson, C.J. 2003. Lithologic mapping in the mountain pass, California area using Advanced Spaceborne thermal Emission and Reflection Radiometer (ASTER) data. Remote Sensing of Environment, 84, 350-366.

Rowan, L.C., Schmidt, R.G. and Mars, J.C. 2006. Distribution of hydrothermally altered rocks in the RekoDiq, Pakistan mineralized area based on spectral analysis of ASTER data. *Remote Sensing of Environment*, 104, pp.74-87.

Sabins, F.F. 1999. Remote sensing for mineral exploration. *Ore Geology Reviews*, 14, 157-183.

Sabins, F. 1997. *Remote sensing principles and interpretation*. 3rd ed. New York: W.H. Freeman and Company, p.494.

Sultan, M., Arvidson, R.E. and Sturchio, N.C. 1986. Mapping of serpentinites in the Eastern Desert of Egypt using Landsat Thematic Mapper data. *Geology*, 14, pp.995-999.

Sultan M., Arvidson R.E., Sturchio N.C. and Guinness, E.A. 1987. Lithologic mapping in arid regions with Landsat thematic mapper data: Meatiq Dome, Egypt. *Geological Society of America Bulletin,* 99(6), pp.748-762.

Yamaguchi, Y. and Naito, C. 2003. Spectral indices for lithologic discrimination and mapping by using the ASTER SWIR bands. *International Journal of Remote Sensing*, 24(22), pp.4311-4323.

Zadeh, M.H., Tangestani, M.H., Roldan, F.V. and Yusta, I. 2014. Sub-Pixel mineral mapping of a porphyry copper belt using EO-1 Hyperion data. *Advances in Space Research*, 53, pp.440-451.

Zhang Tingbin, Yi Guihua, Li Hongmei, Wang Ziyi, Tang Juxing, Zhong Kanghui, Li Yubin, Wang Qin and Bie Xiaojuan. 2016. Integrating Data of ASTER and Landsat-8 OLI (AO) for Hydrothermal Alteration Mineral Mapping in Duolong Porphyry Cu-Au Deposit, Tibetan Plateau, China. *Remote Sensing*, 8, p.890.